Failure prediction of electrolytic capacitors during operation of a switchmode power supply

Amine Lahyani, Pascal Venet, Guy Grellet, Pierre-Jean Viverge

Failure Prediction of Electrolytic Capacitors During Operation of a Switchmode Power Supply

Amine Lahyani, Pascal Venet, Guy Grellet, and Pierre-Jean Viverge

***Abstract*—Electrolytic filter capacitors are frequently responsible for static converter breakdowns. To predict these faults, a new method to set a predictive maintenance is presented and tested on two types of converters.**

The best indicator of fault of the output filter capacitors is the increase of ESR. The output-voltage ripple ΔV_o of the converter increases with respect to ESR. In order to avoid errors due to load variations, ΔV_o is filtered at the switching frequency of the converter. The problem is that this filtered component is not only dependent on the aging of the capacitors, but also on the ambient temperature, output current, and input voltage of the converter. Thus, to predict the failure of the capacitors, this component is processed with these parameters and the remaining time before failure is deduced.

Software was developed to establish predictive maintenance of the converter. The method developed is as follows. First, a reference system including all the converter parameters was built for the converter at its sound state, i.e., using sound electrolytic filter capacitors. Then, all these parameters were processed and compared on line to the reference system, thereby, the lifetime of these capacitors was computed.

***Index Terms*— Aging, electrolytic capacitors, maintenance, power supplies.**

NOMENCLATURE

PS1	Half-bridge dc/dc forward-type converter.
PS2	Zero-current-switched secondary resonant half-wave dc/dc forward-type converter.
ESR	Equivalent series resistance of the capacitor.
L_o	Output smoothing coil of the converter.
V_o	Output voltage.
ΔV_o	Output-voltage ripple.
ΔV_{of}	The component of ΔV_o at the switching frequency of the converter.
I_o	Output current.
Δi	Output-current ripple.
V_i	Input voltage.
T_a	Ambient temperature.
T_c	Case temperature of the electrolytic filter capacitors.
T	Aging temperature.

I. INTRODUCTION

IN VARIOUS electronic equipment, static converters are essential subsystems whose failure leads to the imminent and total stoppage of the equipment.

Manuscript received December 18, 1996; revised March 6, 1998. This work was supported by Centralp Automatismes, Venissieux, France, and ANVAR, France. Recommended by Associate Editor, J. Sarjeant.

The authors are with Cegely Upres A 5005 CNRS, Université Claude Bernard de Lyon, 69622 Villeurbanne-Cedex, France.

Publisher Item Identifier S 0885-8993(98)08311-2.

Because most of the breakdowns in power supplies are accountable to the electrolytic capacitors, a study of the changes in the electrical waveforms due to the wearing out of these capacitors is necessary to set predictive maintenance of the converter.

With the help of two switchmode power supplies using constant and variable switching frequencies, we start this paper by noting the high probability of failure of electrolytic capacitors with respect to the other components.

We then analyze the influence of frequency, temperature, and service life upon the characteristics of the electrolytic capacitors and show the importance of the equivalent series resistance (ESR) in the fault prediction of the capacitors as well as the output-ripple voltage ΔV_o, which depends on ESR [1]–[3].

The first purpose of this study is to show a processing method for output-voltage ripple ΔV_o available even if the converter is submitted to a sudden load variation. Reference [4] gives a process that deals with the full wave rectified and cannot avoid large errors with frequent load variations.

By monitoring the component of the output-voltage ripple ΔV_o at the switching frequency of the converter (denoted by ΔV_{of}), we improve the processing to avoid such errors.

Then, for the two types of converters, a method to predict the failure of the output capacitors is developed as follows.

To begin with, ΔV_{of} is converted into a dc voltage. ΔV_{of} is not only dependent on the aging of the capacitors, but also on the output current, input voltage, and ambient temperature. Thus, these latter parameters are also converted into dc voltages to be processed by software with the use of an acquisition board.

Since ΔV_{of} is a function of the ESR of the electrolytic filter capacitors, ΔV_{of}(ESR) of the converter is determined using sound electrolytic capacitors, with the help of the previous parameters. For aged capacitors, the same function can be used to determine the ESR value knowing the value of ΔV_{of}.

This work presents software that is able to estimate the ESR value of the electrolytic filter capacitors of a converter on line and, therefore, the remaining time before failure.

II. PRESENTATION OF THE CONVERTERS AND THEIR FAILURE CAUSES

Let us consider a half-bridge dc/dc forward-type power supply PS1, as shown in Fig. 1.

The main characteristics of PS1 are as follows.

- The nominal input dc voltage is $V_{\text{in}} = 24$ V.
- The input dc voltage V_i can vary between $V_{i\,\min}$ (18 V) and $V_{i\,\max}$ (33 V).

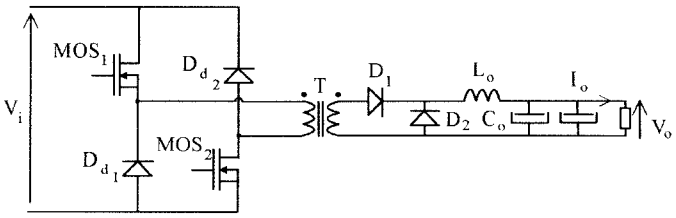

Fig. 1. Diagram of the switchmode power supply PS1.

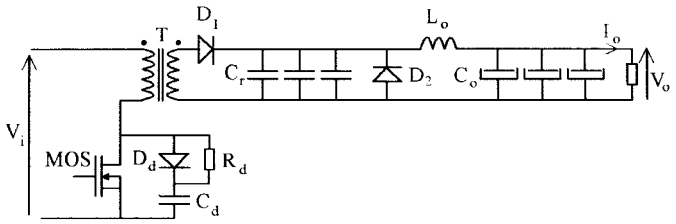

Fig. 2. Diagram of the switchmode power supply PS2.

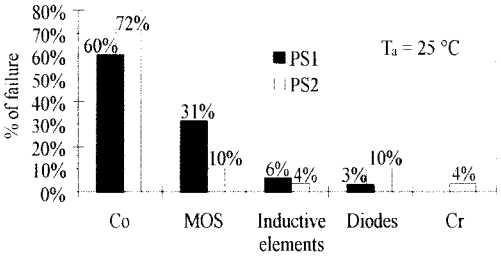

Fig. 3. Distribution of failure for each power component.

- The output dc voltage V_o is equal to 5 V.
- The nominal output current is $I_{\rm on} = 8$ A.
- The output current I_o can vary between zero and $I_{\rm on}$.
- The output filter capacitors are aluminum electrolytic capacitors rated: 2200 μF, 10 V, and 105°C.
- The switching frequency of this converter is 66 kHz.

Let us also consider the zero-current-switched secondary resonant half-wave dc/dc forward-type power supply PS2 as shown in Fig. 2.

- The nominal input dc voltage is $V_{\rm in} = 48$ V.
- The input dc voltage V_i can vary between $V_{i\,\rm min}$ (36 V) and $V_{i\,\rm max}$ (60 V).
- The output dc voltage V_o is equal to 5 V.
- The nominal output current is $I_{\rm on} = 20$ A.
- The output current I_o can vary between $I_{\rm on}/100$ and $I_{\rm on}$.
- The output filter capacitors are aluminum electrolytic capacitors rated: 4700 μF, 10 V, and 105°C.
- C_r are polypropylene capacitors.
- The switching frequency of this converter varies between 10–100 kHz.

Referring to MIL-HDBK 217 F standard [5], the distribution of failures for each component is represented in Fig. 3 at ambient temperature $T_a = 25$°C and under nominal conditions, for both types of converters. The electrolytic capacitors used to smooth the output voltage have the highest probability of failure and are responsible in both cases for more than half of the breakdowns.

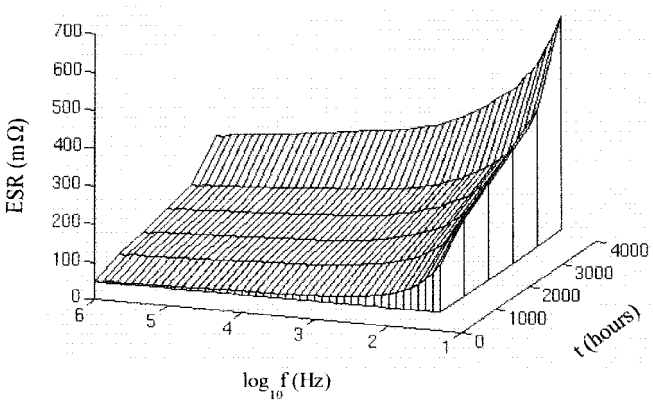

Fig. 4. ESR $= f(t, f)$ measured at $T_a = 25$°C.

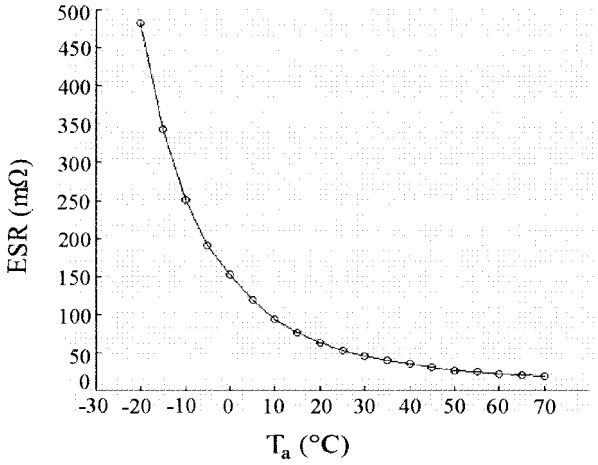

Fig. 5. ESR versus temperature for sound capacitors.

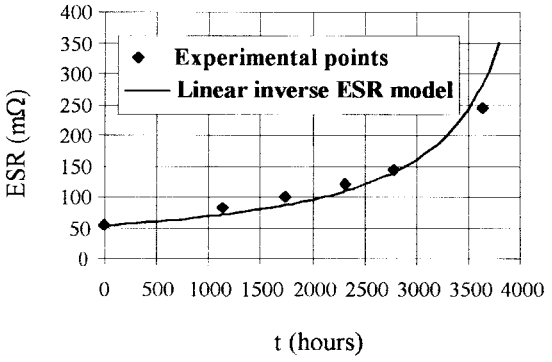

Fig. 6. Aging test of electrolytic capacitors at $T = 105$°C (values measured at $T_a = 25$°C and $f = 66$ kHz).

III. Influence of the Service Life upon the Parameters of the Capacitors

The wearout of aluminum electrolytic capacitors is due to vaporization of electrolyte that leads to a drift of the main electrical parameters of the capacitor. The equivalent series

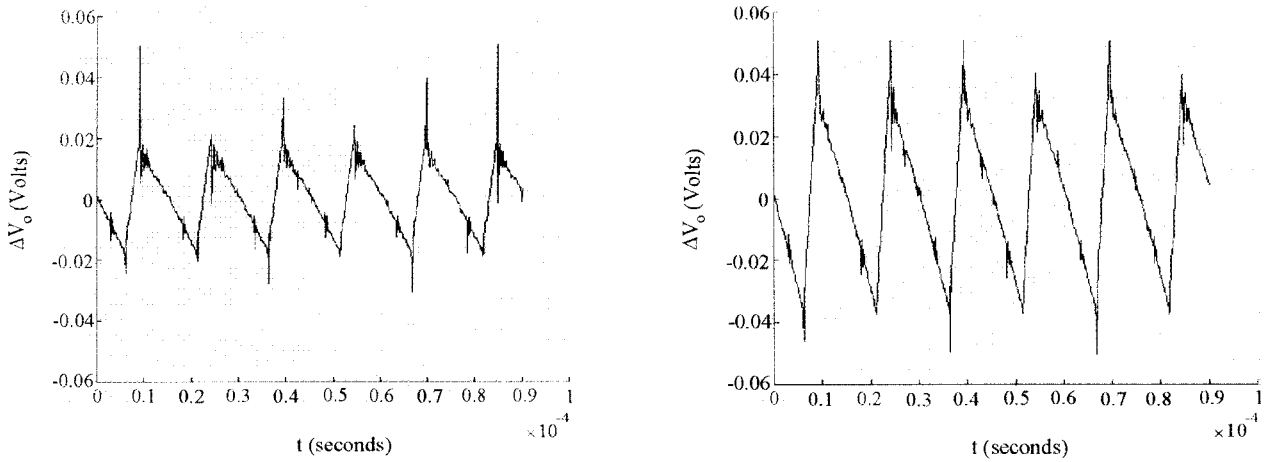

(a) (b)

Fig. 7. Influence on ΔV_o of a faulty capacitor under nominal conditions ($V_i = 24$ V and $I_o = 8$ A). (a) Sound capacitor and (b) aged capacitor.

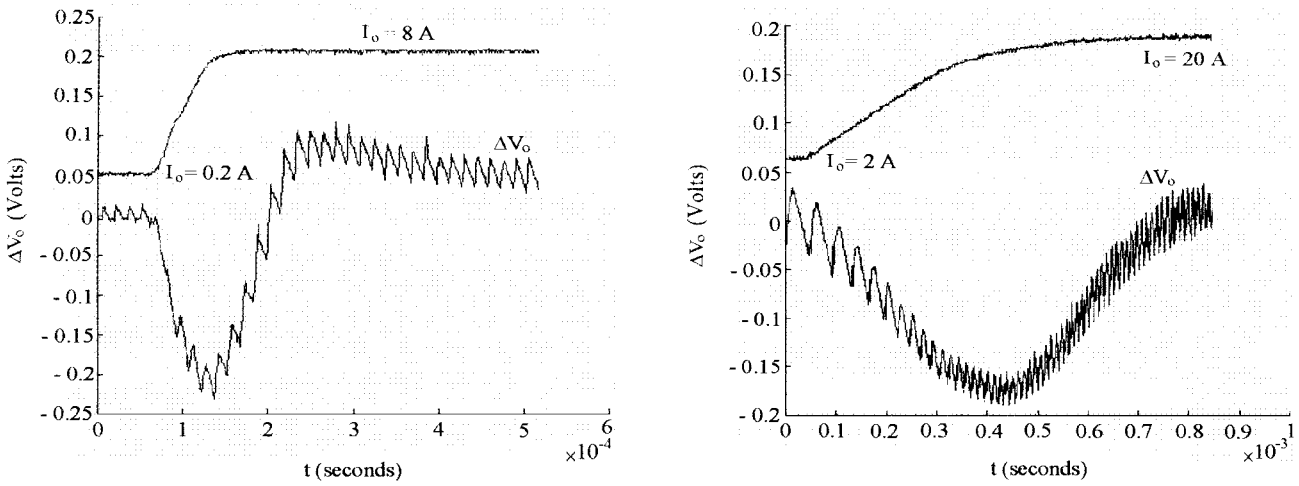

(a) (b)

Fig. 8. Influence of a variable load on ΔV_o for the two converters. (a) Converter PS1 and (b) converter PS2.

resistance ESR increases, and the capacitance C decreases [1], [6], [7]. ESR is the sum of the resistance due to aluminum oxide, electrolyte, spacer, and electrodes (foil, tabbing, leads, and ohmic contacts) [8].

The increase of ESR is interesting since at the switching frequency of the converters, the impedance of the electrolytic capacitors is approximately equal to ESR [3]. In addition, this latter evolution is important since it determines the self-heating and, therefore, indirectly, the capacitor lifetime.

To observe this evolution, we applied to 50 capacitors rated 2200 μF, 10 V, and 105°C an accelerated thermal aging at 105°C and 10 V.

In Fig. 4, for this aging test, we represent the three-dimensional diagram of the ESR, measured at 25°C in a frequency range of 20 Hz to 1 MHz and for the aging times $t = 0$, 1150, 1750, 2300, 2800, and 3650 h.

The ESR is not only dependent on the service life of the capacitor, but at any aging time t, it is inversely affected by temperature [6]. Fig. 5 shows the effect of temperature on ESR for sound capacitors (aging time $t = 0$) rated 2200 μF, 10 V, and 105°C.

For these kinds of capacitors used to filter the output voltage of the converter PS1, a prediction model of ESR at the switching frequency can be determined versus time t. As it will be shown further, the determination of this model is necessary to predict the lifetime of the capacitors online.

Fig. 6 shows the experimental values of the ESR measured at 66 kHz and at $T_a = 25$°C and for the aging test at $T = 105$°C.

For any other aging temperature T', a prediction model of ESR versus time can be deduced from the experimental model at $T = 105$°C. In fact, the relation between the lifetimes t and t', respectively, at the temperatures T and T' (in °C) is given by Arrhenius law

$$\frac{t'}{t} = \exp\left[E.\frac{T - T'}{(T + 273).(T' + 273)}\right] \quad (1)$$

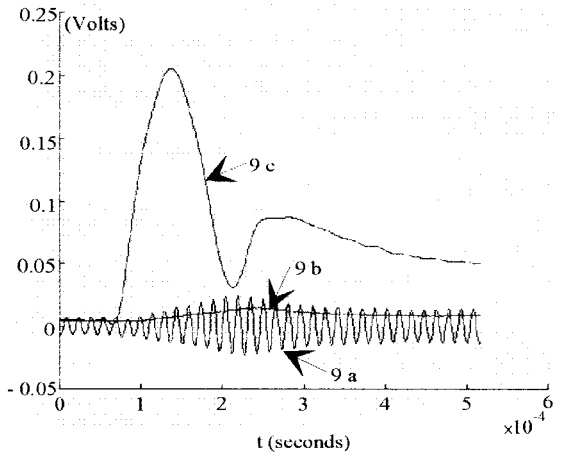

Fig. 9. Processing of ΔV_o for PS1. (a) ΔV_o filtered at the switching frequency of the converter PS1, i.e., 66 kHz. (b) The average rectified signal of (a). (c) The average rectified signal ΔV_o of Fig. 8(a).

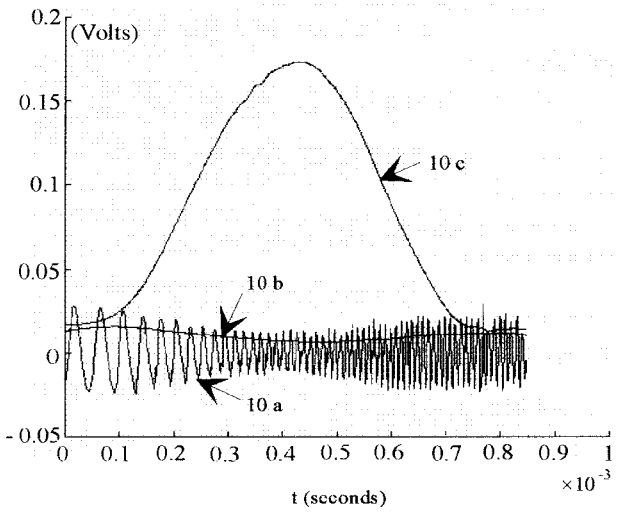

Fig. 10. Processing of ΔV_o for PS2. (a) ΔV_o filtered at the switching frequency of the converter PS2. (b) The average rectified signal of (a). (c) The average rectified signal ΔV_o of Fig. 8(b).

where E is the activation energy/Boltzmann's constant and equals 4700 [9].

The linear inverse model of (2), illustrated in [6], [9], and [10], can also be considered as a good prediction model

$$\frac{1}{\mathrm{ESR}(t)} = \frac{1}{\mathrm{ESR}(0)} \cdot \left(1 - k \cdot t \cdot \exp\left(-\frac{4700}{T+273}\right)\right) \quad (2)$$

where we have the following.

- ESR(t) is the ESR value at time t.
- T is the aging temperature in Celsius degrees.
- t is the aging time.
- ESR(0) is a data representing the ESR value at time $t = 0$.
- k is a constant which depends on the design and the construction of the capacitor.

To have an accurate model, we adjust k by the least-squares method to fit the ESR drift for one type of capacitor.

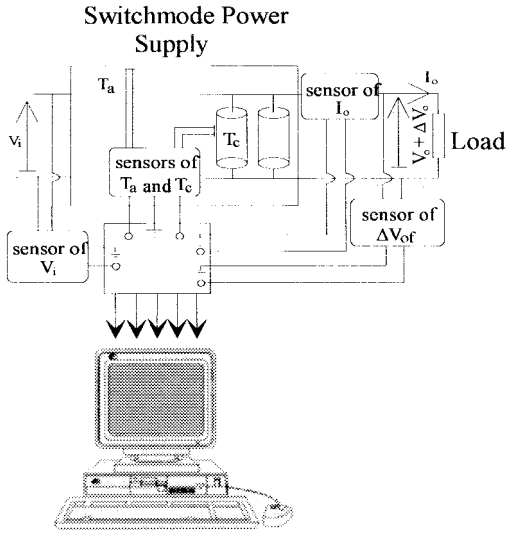

Fig. 11. Sensors and processing system.

We note that in such conditions, the aging temperature T is equal to the case temperature T_c of the capacitor which determines actually the wearout of the latter.

Therefore, one of the foretelling signs of failure is the rise in ESR which is more rapid toward the end of the capacitor life.

IV. Use of the Output-Voltage Ripple to Detect the Electrolytic Capacitor Fault

The only modified waveform of the converter due to an increase in ESR is the output-voltage ripple ΔV_o. In steady-state operations, we represent in Fig. 7 two examples of the waveform ΔV_o using sound capacitors and worn-out ones (ESR twice greater, for instance) for the converter PS1.

Since the switching frequency is constant in the steady-state operation of the converter PS2, the evolution of ΔV_o is similar. The amplitude of ΔV_o is a function of ESR [1], [2].

The main problem then is actually to know which image of the ΔV_o signal should be considered as the best one for the fault prediction method.

We suggest the use of the filtered Fourier component at the switching frequency of the converter (ΔV_{of}). Indeed, compared to the average rectified signal of ΔV_o, which can be taken in such cases [4], the new method is more realistic [11].

Suppose that PS1 is driven at a switching mode between $I_o = 2$, 5% I_{on} and $I_o = 100\%$ I_{on} and that PS2 is driven at a switching mode between $I_o = 10\%$ I_{on} and $I_o = 100\%$ I_{on}, then the output-voltage ripple ΔV_o presents a transient as shown in Fig. 8(a) (converter PS1) and (b) (converter PS2).

Figs. 9 and 10 show the signal filtered by a bandpass filter centered on the switching frequency of the converter [curves 9a for PS1 and 10a for PS2] and its average rectified value [curves 9b for PS1 and 10b for PS2] and the average rectified original signal [curves 9c for PS1 and 10c for PS2].

We notice that a surge value of ΔV_o occurs at the moment of the load change that is completely detected by the signals 9c and 10c, but that is much reduced in the signals 9b and 10b.

This means that the prediction system using curves 9c and 10c is subjected to a sudden increase in the image of ΔV_o, and

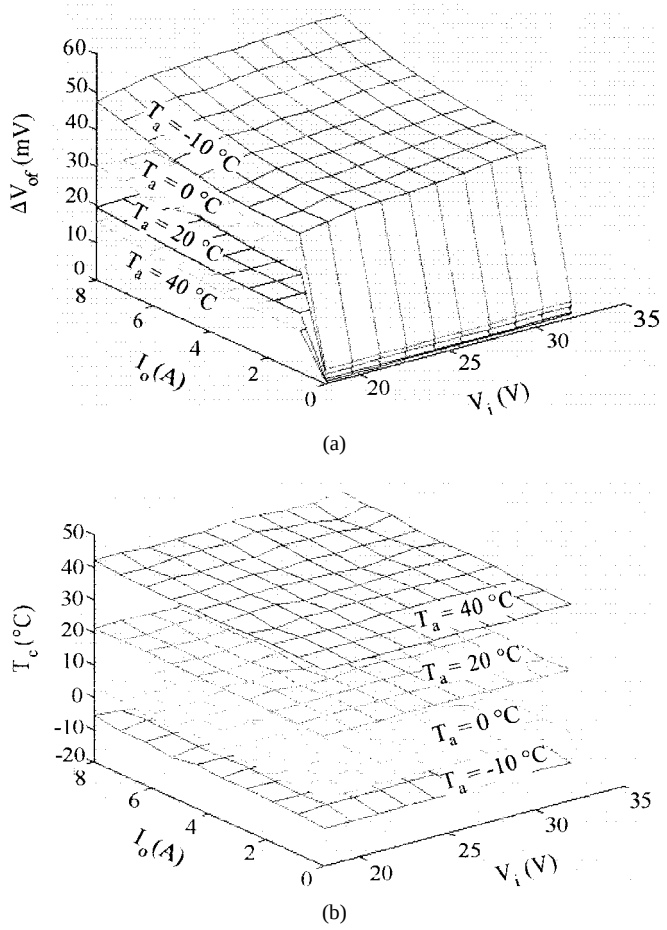

Fig. 12. Diagram of the experimental functions ΔV_{of} and $T_c = f(I_o, V_i, T_a)$ for sound capacitors. (a) Component ΔV_{of} of the output voltage at the switching frequency of the converter and (b) case temperature T_c.

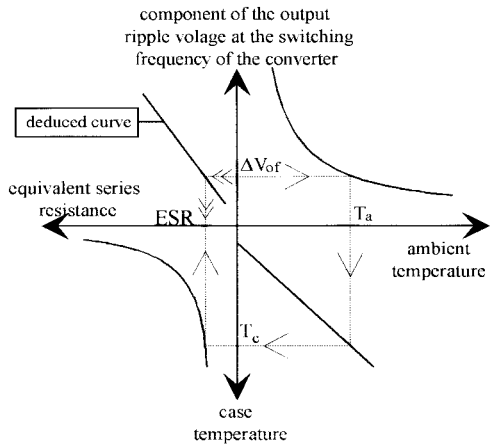

Fig. 13. Computation of ΔV_{of}(ESR) for a sound capacitor with the use of $\Delta V_{of} = f(T_a)$, $T_c = f(T_a)$, and ESR $= f(T_c)$.

then a fault may be signaled improperly at this time, while the curves 9b and 10b show a negligible variation in the image of ΔV_o considered.

For the half-bridge dc/dc forward-type power supply PS1 of Fig. 1, which works at constant switching frequency (66 kHz), the measurement of ΔV_{of} is obtained by a bandpass filter centered on 66 kHz and by a stage that rectifies and amplifies the filtered waveform and gives a dc image of ΔV_{of} [12].

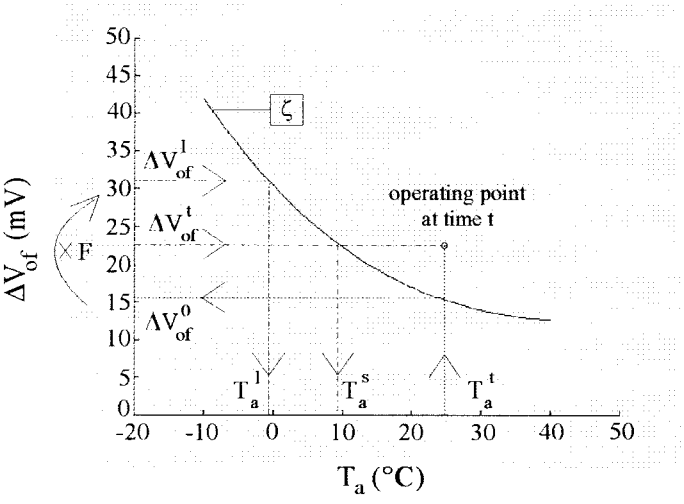

Fig. 14. $\Delta V_{of} = f(T_a)$ for $I_o = I_{\rm on}/2 = 4$ A and $V_i = V_{\rm in} = 24$ V.

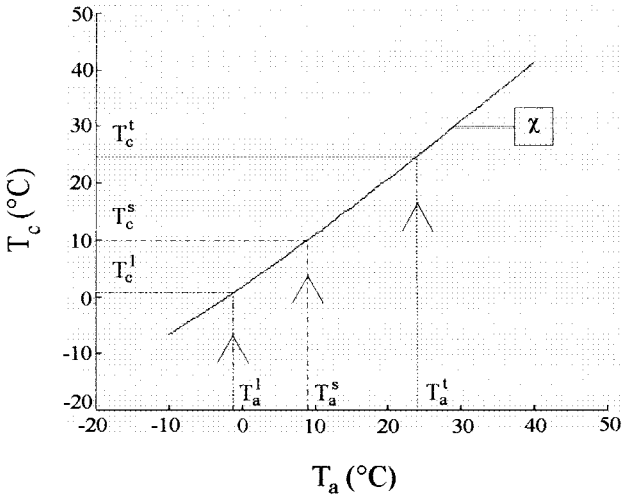

Fig. 15. $T_c = f(T_a)$ for $I_o = I_{\rm on}/2 = 4$ A and $V_i = V_{\rm in} = 24$ V.

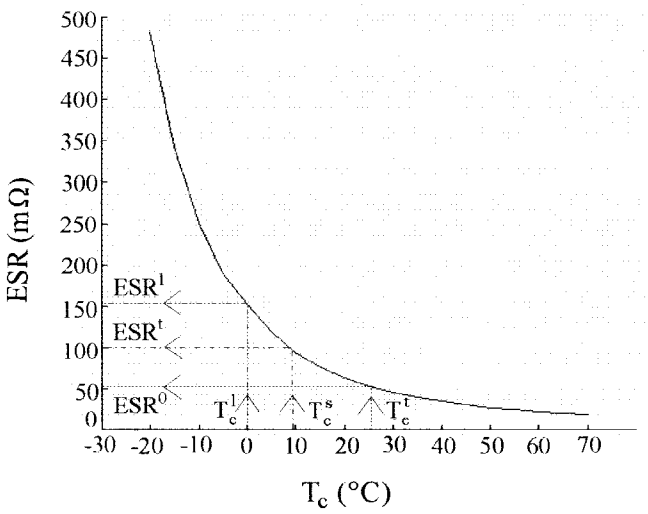

Fig. 16. Determination of the capacitors state using the law ESR $= f(T_c)$.

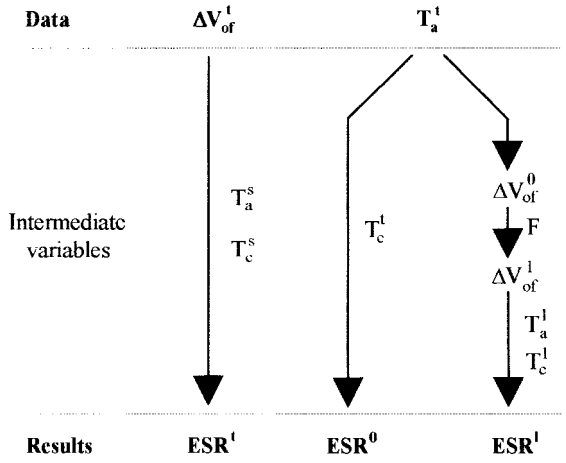

Fig. 17. Computation method of ESR^0, ESR^t, and ESR^l.

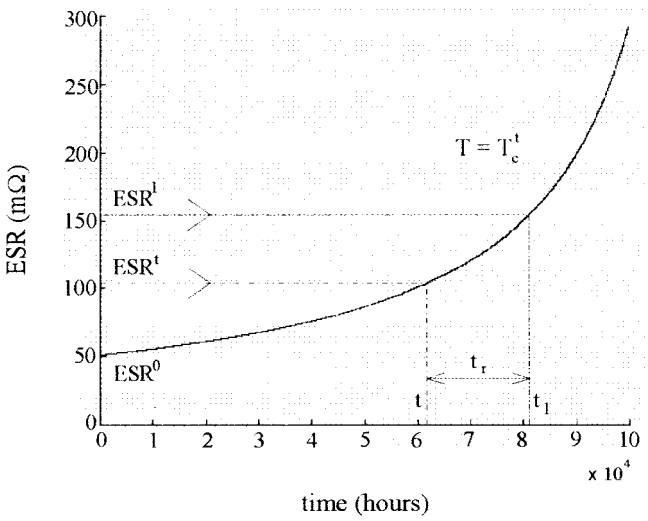

Fig. 18. Computation of the remaining time t_r before failure using the law ESR $= f(t, T)$ at $T = T_c^t$.

For the zero-current-switched secondary resonant half-wave dc/dc forward-type power supply PS2 of Fig. 2, the frequency of ΔV_{of} varies in the same range as the switching frequency, i.e., between 10–100 kHz. The system to be designed must give a faithful image of ΔV_{of} in frequency and amplitude without affecting the original signal.

The circuit used is a selective bandpass filter with a center frequency controlled by a voltage [13]. By applying an amplified image of ΔV_o to the filter input and setting the center frequency f_c equal to the switching frequency, we obtain as output the amplified image of ΔV_{of} [3].

V. The Real-Time Prediction of the Electrolytic Filter Capacitor Fault

The failure of the output electrolytic filter capacitor in a static converter is characterized by the increase in the value of ESR due to the converter operation during a time t, at a temperature T.

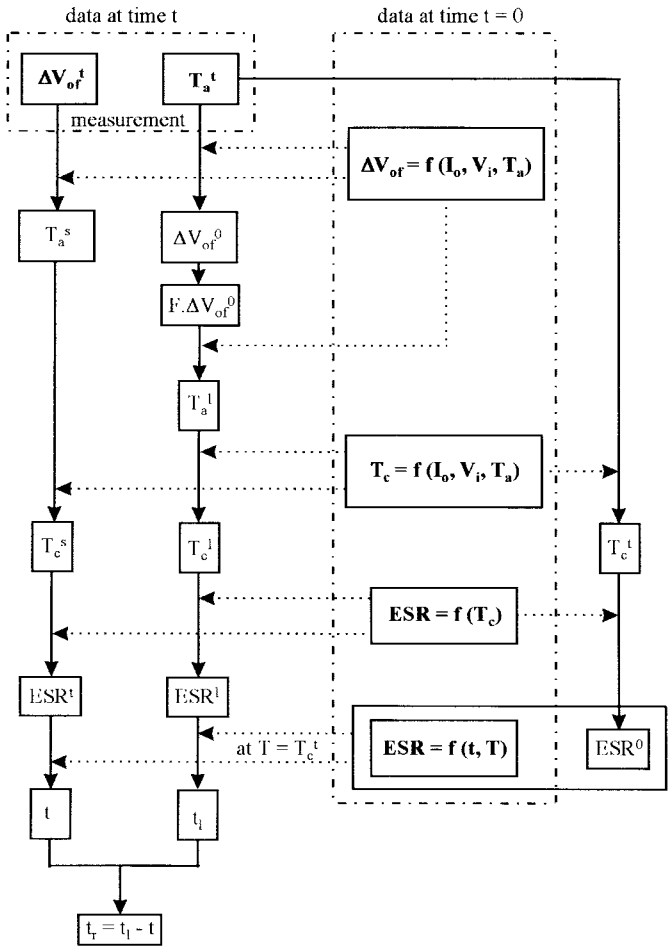

Fig. 19. Block diagram of the software.

To determine the ESR and the time before the failure of the capacitor, we must proceed to a measurement of the case temperature T_c of the latter as well as the component ΔV_{of} of the output-voltage ripple ΔV_o. The temperature T_c takes account of the ambient temperature and the heating produced by the output current ripple [7], [14], [15].

The sensors and the processing system of Fig. 11 are used to convert the parameters of the converter (I_o, V_i, T_a, T_c, ΔV_{of}) into dc voltages between 0–10 V. All the dc signals are then processed by software.

Since ΔV_{of} and T_c depend on the output current I_o, input voltage V_i, and ambient temperature T_a, we will obtain at first an experimental acquisition of the functions $\Delta V_{of} = f(I_o, V_i, T_a)$ and $T_c = f(I_o, V_i, T_a)$ for a converter using sound electrolytic filter capacitors (time $t = 0$) with the use of the system of Fig. 11. We make then a reference system for ΔV_{of} and T_c.

For a given time $t \neq 0$ and for a given operating mode (I_o, V_i, T_a), the software reads continuously the measurements of the parameters ΔV_{of} as well as I_o, V_i, and T_a. The case temperature T_c is not measured directly at the surface of the capacitor, but deduced by the software from the reference system built at $t = 0$. This method reduces the number of sensors if many electrolytic capacitors are used or if other electronic components of the converter are monitored.

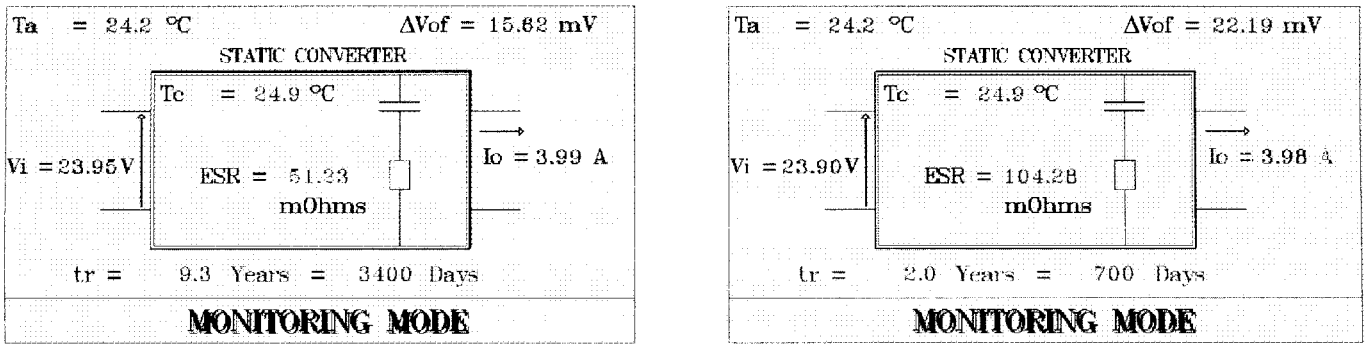

Fig. 20. Results obtained by the software in the case of a converter using sound and worn electrolytic filter capacitors.

The measured ΔV_{of} at $t \neq 0$ is then compared to ΔV_{of} at $t = 0$. Therefore, the ESR value as well as the remaining time before failure are calculated.

The detailed processing method to predict the failure of capacitors is presented now for the converter PS1, but the same method can be applied to the converter PS2.

A. Acquisition of $(\Delta V_{of}, T_c) = f(I_o, V_i, T_a)$ *at* $t = 0$

The electrolytic filter capacitors of PS1 are identical. They have approximately the same case temperature T_c and therefore identical worn state versus time and temperature.

To build a reference system of T_c and ΔV_{of}, the software automatically drives PS1 into different operating modes by varying simultaneously step by step:

- I_o from 0 A to $I_{\rm on}$ (8 A) with the use of a controlled dc electronic load;
- V_i from $V_{i\,\rm min}$ (18 V) to $V_{i\,\rm max}$ (33 V) with the use of a controlled dc power supply;
- T_a from -10°C to $+40$°C.

So, the built vectors I_o, V_i, and T_a and matrices T_c and ΔV_{of} are the reference data stored by the software and used later in the real-time monitoring.

In Fig. 12, we represent T_c and ΔV_{of} versus I_o and V_i at four different ambient temperatures (40, 20, 0, and -10°C).

We observe an increase in ΔV_{of} when the ambient temperature decreases which is due to a rise in the ESR (Fig. 5).

The temperatures T_c and T_a are imposed by a climate chamber containing the converter PS1.

B. Processing of the Different Signals at Time $t \neq 0$

1) Method: To compute the ESR value of an electrolytic filter capacitor, the method applied is as follows.

1) At first, the function $\Delta V_{of} = f(T_a)$, for given I_o and V_i is deduced from the reference system of Fig. 12(a).
2) Second, the function $T_c = f(T_a)$ for the same I_o and V_i is deduced from the reference system of Fig. 12(b).
3) Finally, knowing the evolution law ESR $= f(T_c)$ for a sound capacitor (Fig. 5), we can deduce ΔV_{of} versus ESR for a sound capacitor and for I_o and V_i as shown in Fig. 13.

We notice that the three functions described previously are constituted of discrete measures. The cubic spline method is used for interpolation.

We notice that ΔV_{of}(ESR) is actually almost independent of the ambient temperature T_a. In fact, the impedance Z of the capacitor is almost equal to ESR at the switching frequency of PS1 [3]. The current ripple Δ_i across the capacitor is fixed by the output smoothing coil L_o of Fig. 1, which is almost independent of T_a and the output-voltage ripple is given by

$$\Delta V_o = Z.\Delta i \approx \text{ESR}.\Delta i. \tag{3}$$

The variation law of ΔV_{of} versus ESR depends only on I_o and V_i. It is then determined for a sound capacitor (Fig. 13) and can be used to compute the ESR value of a worn capacitor by knowing only I_o, V_i, and the value of ΔV_{of}.

2) Utilization of $\Delta V_{of} = f(I_o, V_i, T_a)$*:* We suppose that at time $t \neq 0$, the converter is driven into the operating mode ($I_o = I_{\rm on}/2 = 4$ A, $V_i = V_{\rm in} = 24$ V). The measured values of ΔV_{of} and T_a at that time are ΔV_{of}^t and T_a^t. The curve ζ of Fig. 14 is the reference curve of $\Delta V_{of} = f(T_a)$ deduced by the software from the reference system of Fig. 12(a).

We notice that ΔV_{of}^t and T_a^t does not join the curve ζ because the electrolytic filter capacitors are worn.

The program computes on line the next values.

T_a^s Temperature corresponding to the real value ΔV_{of}^t on the curve ζ. T_a^s would be the ambient temperature if the capacitors were sound and if $\Delta V_{of} = \Delta V_{of}^t$.

ΔV_{of}^0 Output-voltage ripple corresponding to the real measured temperature T_a^t on the curve ζ. ΔV_{of}^0 would be the value of ΔV_{of} if the filter capacitors were sound and if $T_a = T_a^t$.

The user of the software must define the limit of the correct running of the converter by entering a factor F that shows the limit value ΔV_{of}^l permitted at the operating mode (I_o, V_i, T_a^t)

$$\Delta V_{of}^l = F.\Delta V_{of}^0. \tag{4}$$

The limit ambient temperature T_a^l is then deduced from ΔV_{of}^l by the curve ξ. It would represent the temperature if sound filter capacitors were used and if $\Delta V_{of} = \Delta V_{of}^l$.

We remark that if the correct operating limit, defined by the user is large, the ΔV_{of}^l value can exceed the limit of the

curve ζ, this is why it is better to build the reference system for a wide range of ambient temperatures and mainly for the negative values.

We then compute and store three temperatures T_a^t, T_a^s, and T_a^l, on line, to be used in the next step.

3) Utilization of $T_c = f(I_o, V_i, T_a)$: The software determines for $I_o = 4$ A and $V_i = 24$ V the curve χ (Fig. 15) that represents the case temperature T_c versus the ambient temperature T_a deduced from the reference system of Fig. 12(b).

From T_a^t, T_a^s, and T_a^l, the program deduces the values of:

- T_c^t real case temperature at time t;
- T_c^s case temperature corresponding to T_a^s and then to ΔV_{of}^t if sound capacitors were used;
- T_c^l limit case temperature corresponding to T_a^l and ΔV_{of}^l if sound capacitors were used.

4) Utilization of ESR $= f(T_c)$: For sound electrolytic capacitors used to filter the output voltage, the variation of ESR versus the case temperature is known (Fig. 5). This function is used to determine on line, the state of the filter capacitors as shown in Fig. 16.

From T_c^t, T_c^s, and T_c^l, the software calculates:

- ESR^0 ESR value of a sound capacitor at ambient temperature T_a^t and case temperature T_c^t;
- ESR^t real ESR value at time t deduced from T_c^s as explained in the method of V. B. 1;
- ESR^l limit value of ESR corresponding to the right operating mode of the converter.

To sum up, we represent in Fig. 17 the method used to compute ESR^0, ESR^t, and ESR^l from the data ΔV_{of}^t and T_a^t at time t.

5) Utilization of ESR $= f(t, T)$: The converter is working at ambient temperature T_a^t and the temperature of the filter capacitors case is equal to T_c^t.

Using the law $\text{ESR} = f(t, T)$ (Fig. 6), where T is set to T_c^t and $\text{ESR}(0)$ is equal to ESR^0 calculated in Section V-B-4, the program computes, as shown in Fig. 18, the remaining time before failure if we assume that it will keep the same operating mode until the complete failure of the capacitors.

C. Synthesis of the Processing Method

The block diagram illustrated by Fig. 19 shows the method used to predict electrolytic capacitors failure.

VI. Results

The predicted values concerning the failure time of the converter tested, seems to be confirmed by the industrial users.

Fig. 20 shows the results of the monitoring software for sound capacitors ($\text{ESR} = 51$ mΩ) and worn capacitors ($\text{ESR} = 104$ mΩ). The increase permitted for ΔV_{of} is 100% ($F = 2$).

VII. Conclusion

In static converters, the increase in the ESR in the output electrolytic filter capacitors is the best fault signature of the latter.

The output-voltage ripple ΔV_o increases with respect to ESR, and this is why it is monitored to predict the failure of the electrolytic capacitors.

As static converters work most of the time at variable load, the best image of the output voltage to predict the failure of electrolytic filter capacitors is the filtered signal at the converter switching frequency. In fact, this signal gives a faithful value of ΔV_o either at constant load or at variable load and avoids the sudden increase in transient values of ΔV_o that leads to a wrong predicted lifetime of the electrolytic capacitor.

The amplitude of this filtered signal versus ESR is determined for a converter using sound filter capacitors by varying other system parameters such as input voltage, output current, and ambient temperature.

The lifetime of the converter is then continuously predicted by monitoring on line all the converter parameters.

References

[1] K. Harada, A. Katsuki, and M. Fujiwara, "Use of ESR for deterioration diagnosis of electrolytic capacitors," *IEEE Trans. Power Electron.*, vol. 8, no. 4, pp. 355–361, 1993.

[2] P. Venet, H. Darnand, and G. Grellet, "Detection of faults of filter capacitors in a converter. Application to predictive maintenance," in *INTELEC Proc.*, 1993, vol. 2, pp. 229–234.

[3] P. Venet, "Surveillance d'alimentations á découpage. Application á la maintenance prédictive," Master's thesis, Claude Bernard University, Lyon, France, 1993.

[4] K. Harada, "Life detector for smoothing capacitor," Japanese Patent 63 81 277.

[5] Military Handbook 217 F, "Reliability prediction of electronic equipment," Feb. 28, 1995.

[6] M. L. Gasperi, "Life prediction model for aluminum electrolytic capacitors," in *IEEE IAS Conf. Proc.*, 1996, pp. 1347–1351.

[7] B. Alvsten, "Electrolytic capacitors theory and application," RIFA Electrolytic Capacitors, Sweden, 1995.

[8] United Chemi-Con Inc., "Understanding aluminum electrolytic capacitors," Catalog U 7002, 2nd ed., 1995.

[9] G. E. Rhoades and A. W. H. Smith, "Expected life of capacitors with nonsolid electrolyte," in *34th Component Conf. Proc.*, 1984, pp. 156–161.

[10] J. A. Jones and J. A. Hayes, "The parametric drift behavior of aluminum electrolytic capacitors: An evaluation of four models," in *1st European Capacitor and Resistor Technology Proc.*, Brighton, U.K., 1987, pp. 171–179.

[11] P. Venet, A. Lahyani, P. J. Viverge, and G. Grellet, "Use of the output voltage of a switchmode power supply to predict failure of filtering electrolytic capacitors," in *EPE'97 Proc.*, 1997, vol. 2, pp. 978–982.

[12] B. E. Noltingk, *Instrumentation Reference Book.* Kent, U.K.: Butterworth, 1990.

[13] L. Tran Tien, *Electronique des systèmes de mesures: Mise en oeuvre des procédés analogiques et numériques.* Paris, France: Masson, 1984.

[14] J. L. Stevens, J. D. Sauer, and J. S. Shaffer, "Improved thermal model for large can aluminum electrolytic capacitors: An empirical approach," in *15th Capacitor and Resistor Technology Symp. Proc.*, 1995, pp. 56–61.

[15] L. J. Hart and D. Scoggin, "Predicting electrolytic capacitor lifetime," *Powertechniques Mag.*, pp. 24–29, Oct. 1987.

Amine Lahyani was born on October 30, 1970 in Sfax, Tunisia. He received the Engineer and the Post Graduate (DEA) degrees in electrical engineering from the National Polytechnic Institute of Grenoble (INPG), France, in 1994 and the Ph.D. degree in electrical engineering from the Claude Bernard University Lyon I—Center of Electrical Engineering of Lyon (CEGELY), France, in 1998.

His main research interest includes power electronics, especially the diagnosis of static converters.

Pascal Venet was born in Aix-Les-Bains, France, on March 16, 1965. He received the M.Sc. degree in 1990 and the Ph.D. degree in electrical engineering in 1993, both from the Claude Bernard University Lyon I (UCBL), France.

He was a Research and Development Engineer at Centralp—Automatismes, France. Since 1995, he has been an Assistant Professor at UCBL. His current research interests include static converters fault diagnostics and aging of discrete components.

Guy Grellet was born in France in 1937. He received the Dipl.-Ing. degree from "Ecole Centrale de Lyon" (ECL) in 1961 and the Ph.D. degree in electrical engineering in 1977 from the University Claude Bernard—Lyon I (UCBL), France.

From 1962 to 1978, he was "Maître de Conférence" at ECL/France. He joined "Compagnie Electromécanique" (CEM) from 1978 to 1980, where he was involved in R&D of high-speed electrical machines. Since 1981, he has been a Professor at UCBL. From 1985 to 1997, he was the Director of "Laboratoire d'Electrotechnique et d'Electronique de Puissance—UCBL." His research interests include rotating alternative current machines and power electronics and, particularly, modelization of parasitic phenomena, losses, and fault diagnosis.

Pierre-Jean Viverge was born in Dijon, France, in 1965. He received the B.S., M.S., and Ph.D. degrees in electrical engineering from the National Applied Sciences Institute of Lyon (INSA—Lyon), France.

He is currently an Associate Professor at INSA. He joined the Center of Electrical Engineering of Lyon (CEGELY—CNRS) in 1989. From 1989 to 1995, his research was in high-temperature electronics. Currently, his research interests include diagnostics in power electronics.